Measuring Gravitational Lensing Flexions with an Analytic Image Model

B. Cain, P. Schechter, & M. Bautz (astro-ph/1103.0551)

Massachusetts Institute of Technology

UC DAVIS UNIVERSITY OF CALIFORNIA

Abstract

We present a new technique for measuring gravitational lensing flexions (second-order weak lensing effects): the Analytic Image Model (AIM) method. By parametrizing both the unlensed surface brightness profile and the lensing transformation with analytic functions, we optimize our model image to constrain the flexions acting on each lensed galaxy image. We fix the shear parameters to ensure convergence, taking advantage of the shear/ellipticity degeneracy. Simulations verify that the AIM method accurately recovers flexions, and we apply the AIM method to HST images of Abell 1689 and detect small-scale mass substructure in the cluster.

Second-Order Weak Lensing

The second-order lens equation includes the additional lensing fields $\mathcal{F} = \nabla\kappa$ and $\mathcal{G} = \nabla\gamma$, called 1-flexion and 3-flexion, respectively, for their rotation symmetries. As usual, the observable lensing fields are those which are invariant to the mass-sheet degeneracy. These are the reduced shear and flexions:

$$g = \frac{\gamma}{1-\kappa}, \quad \Psi_1 = \frac{\mathcal{F}}{1-\kappa}, \quad \Psi_3 = \frac{\mathcal{G}}{1-\kappa}$$

These three complex fields describe the quadratic lensing transformation from the image plane (θ) to a fiducial source plane (β):

$$\beta = \theta - g\theta^* - \frac{1}{4}\Psi_1^*\theta^2 - \frac{1}{2}\Psi_1\theta\theta^* - \frac{1}{4}\Psi_3(\theta^*)^2.$$

Flexions are significant to the transformation in regions where $\kappa, |\gamma| \not\ll 1$.

Analytic Image Model

In contrast to the HOLICs and shapelets methods, we fit each observed background galaxy with an elliptical Gaussian surface brightness profile, lensed to second order, and minimize the figure of merit:

$$\chi^2(P) = \sum_k \frac{\left(I_{\rm data}(\theta^{(k)}) - I_{\rm model}(\theta^{(k)}; P)\right)^2}{\sigma(\theta^{(k)})^2}$$

to find the best-fit parameter vector P. The model includes 6 intrinsic shape parameters, 6 lensing parameters, background, and convolution with a circular, Gaussian PSF. The minimization is performed in IDL using `MPFIT`, a robust implementation of the Levenberg-Marquardt non-linear minimization algorithm.

The AIM method returns flexions, error estimates, and full correlation matrices. These are important tools for evaluating the quality of flexion estimates and appropriately weighting mass reconstructions. Individual error estimates for all flexion parameters of each analyzed image is a new feature for flexion measurement methods. Tests using fits to a wide variety of simulated data images validate the AIM method.

Ellipticity/Shear Degeneracy

Ellipticity and shear are degenerate:

$$\epsilon_{obs} = \frac{\epsilon + g}{1 + \epsilon g^*} \text{ for } |g| < 1; \quad \frac{1 + \epsilon^* g}{\epsilon^* + g^*} \text{ for } |g| > 1$$

For each image, we fix the shear parameters to an observationally-motivated model values and measure the flexion fields. The flexions are not directly coupled to the shear or the ellipticity (Ψ_1 is spin-1 and Ψ_3 is spin-3, while ϵ and g are both spin-2), so errors in the shear model are absorbed into the (unobservable) intrinsic ellipticity. The shear model can then be updated if necessary using unlensed ellipticity correlations and/or integrated flexions.

Lensing Field Effects

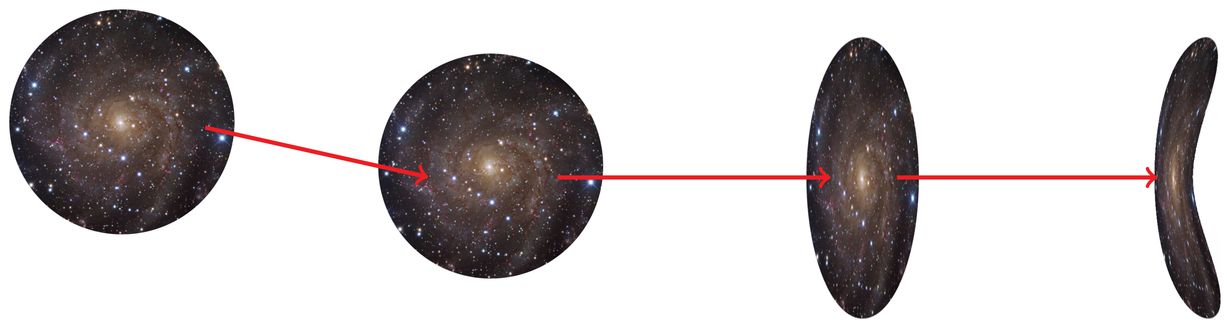

Zeroeth-Order Lensing	First-Order Lensing	Second-Order Lensing
Displacement	Magnification/Shear	Flexions
$\alpha = \nabla\psi$	$\kappa = \frac{1}{2}\nabla^*\alpha$	$\mathcal{F} = \nabla\kappa = \nabla^*\gamma$
	$\gamma = \frac{1}{2}\nabla\alpha$	$\mathcal{G} = \nabla\gamma$

Application of AIM to A1689

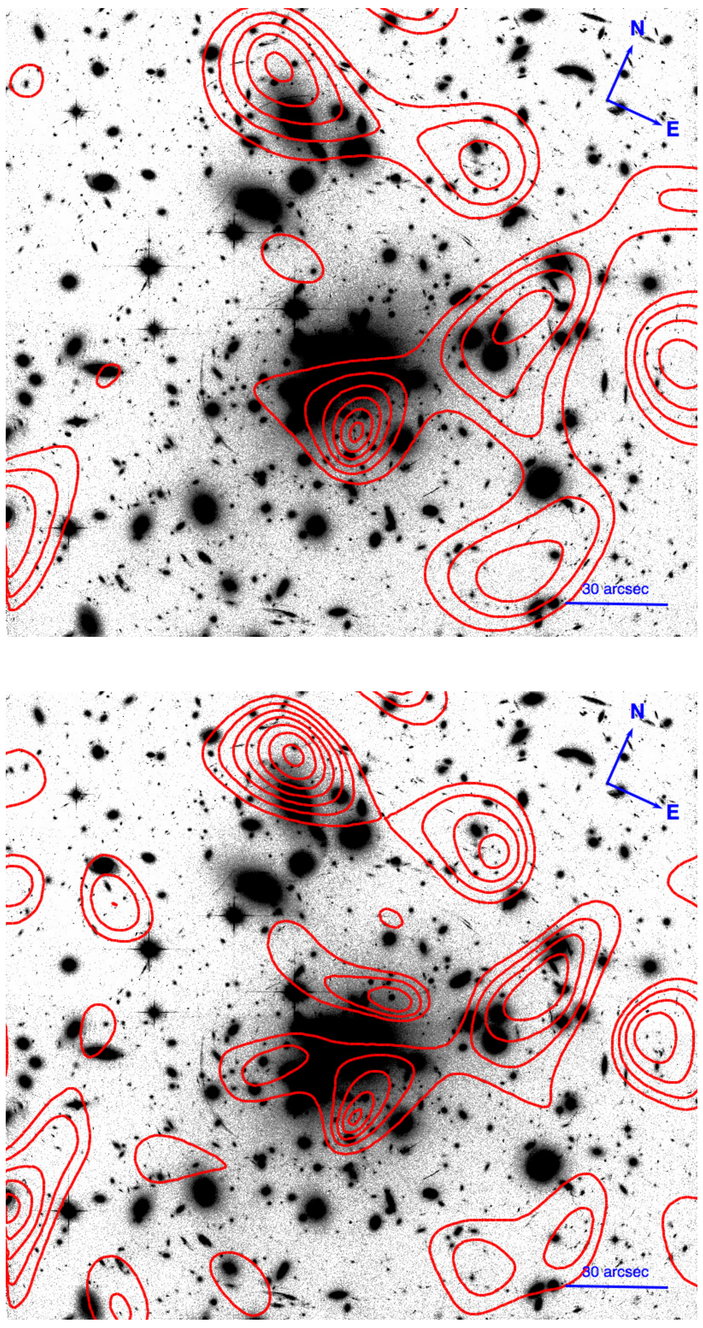

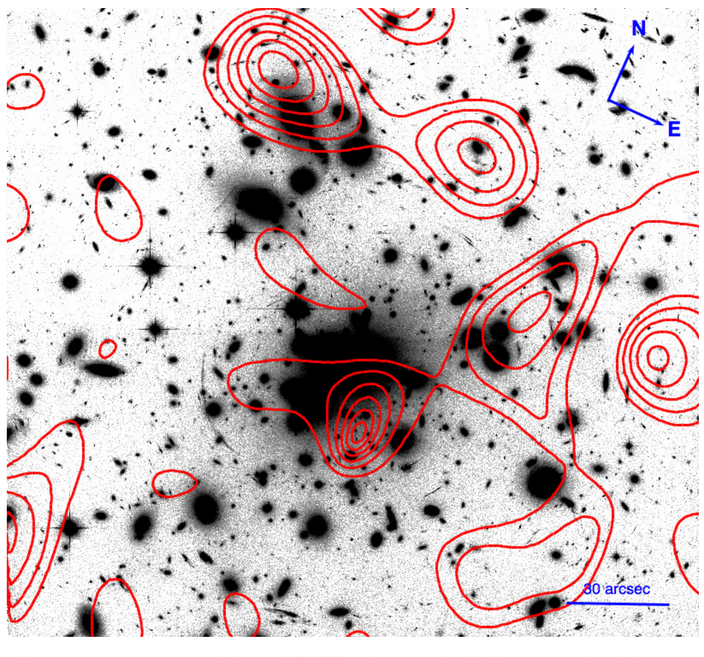

Contours of $K_{\rm ap}$ SNR in A1689 overlaid on an optical HST image. Contours start at $K_{\rm ap}/\sigma_{K_{\rm ap}} = 5$ and increase in steps of 2. Each image uses a different polynomial flexion kernel:

$$Q(r) = A_n\, r \left(1 - \frac{r^2}{R^2}\right)^{n+1}$$

Above left: $n = 3$; above right: $n = 5$; left: $n = 7$; $R = 60''$. Higher filter indices include more noise as fewer galaxies are included by the kernel. Structures are detected with multiple filters, but small structures are more smoothed out at lower indices, as would be expected. Missing data when the kernel extends past the field edge produces spurious signals near the borders.

1-Flexion $\Rightarrow$ Structure

1-Flexion is sensitive to convergence gradients:

$$\Psi_1(\theta) = -\nabla \ln|1 - \kappa(\theta)|.$$

To measure mass structure, we define

$$K(\theta) = -\ln|1 - \kappa(\theta)|$$

and an integrated "mass" statistic $K_{\rm ap}$:

$$K_{\rm ap}(\theta) = \int_{|r|<R} K(\theta + r)\, W(|r|)\, d^2r.$$

W is an aperture window function with a corresponding flexion kernel Q. $K_{\rm ap}$ is related to the radial flexion components:

$$K_{\rm ap}(\theta) = \int_{|r|<R} \Psi_1(\theta + r) \cdot \hat{r}\, Q(|r|)\, d^2r.$$

We calculate $K_{\rm ap}$ from our flexion measurements in A1689, and create maps of $K_{\rm ap}/\sigma_{K_{\rm ap}}$ by randomly varying the flexion measurements by the AIM-determined error estimates and recalculating $K_{\rm ap}$. This technique is a modification of the Leonard et al. (2011) reconstruction method. More quantitative measurements of the substructure require additional investigation into the systematic effects of the measurement.

References/Acknowledgements

Bertin & Arnouts 1996, A&AS, 117, 393. ◇ Goldberg & Leonard 2007, ApJ, 660, 1003. ◇ Leonard et al. 2011, MNRAS, in press. ◇ Markwardt 2008, ASP Conf. Series, Vol. 30. ◇ Okura et al. 2008, ApJ, 680, 1. ◇ Peng et al. 2009, ApJ, 701, 1283. ◇ Schneider & Er 2008, A&A, 485, 363. ◇ Velander et al. 2011, MNRAS, in press.

This work was supported by funding from NASA through SAO Award Number 2834-MIT-SAO-4018 issued by the Chandra X-Ray Observatory Center, operated by the Smithsonian Astrophysical Observatory for and on behalf of NASA under contract NAS8-03060; and through grant HST-GO-11099 from the Space Telescope Science Institute (STScI), operated by AURA, Inc., under NASA contract NAS5-26555 and NNX08AD79G. These results use observations made with the Hubble Space Telescope, obtained from the Hubble Legacy Archive.